



ISSN Print: 2394-7500
 ISSN Online: 2394-5869
 Impact Factor: 5.2
 IJAR 2017; 3(7): 1006-1010
 www.allresearchjournal.com
 Received: 03-05-2017
 Accepted: 04-06-2017

Bandhan Sharma
 Department of Physics, Govt.
 College for Women Parade,
 Jammu. (Autonomous
 College), Jammu and Kashmir,
 India

Structure-activity-relationship and crystallographic analysis of 9-hydroxy-2-(2-hydroxypropan-2-yl)-2,3-dihydro-7H-furo[3,2-g]benzopyran-7-one

Bandhan Sharma

Abstract

The title compound $C_{14}H_{14}O_5$, is a furanocoumarin [systematic name: 9-hydroxy-2-(2-hydroxypropan-2-yl)-2,3-dihydro-7H-furo[3,2-g]benzopyran-7-one], which was isolated from the seeds of *Apiumgraveolens* (Umbelliferae), a weed cultivated in several parts of India. The compound crystallizes into monoclinic space group C2 with unit cell parameters $a = 24.616(8) \text{ \AA}$, $b = 8.186(3) \text{ \AA}$, $c = 6.632(2) \text{ \AA}$, $\beta = 103.99(2)^\circ$, $Z = 4$. The structure was refined by full matrix least-squares to a final R value of 0.0356 for 2216 observed reflection. The molecules are linked by O-H...O hydrogen bonds into chains and these chains are linked into sheets by C-H...O hydrogen bonds. There are also $\pi \dots \pi$ interactions among the molecules which links the sheet into supramolecular structure. Structure activity predictions have been identified on the basis of structural fragments. In this compound the value of P_a (Probability of activity) is very large as compared to P_i (Probability of inactivity) for Antioxidant, Anti-inflammatory and Respiratory analeptic which shows the positive influence of these descriptions.

Keywords: Crystal structure, Furanocoumarin, hydrogen bond, $\pi \dots \pi$ interaction, supramolecular structure

1. Introduction

In Coumarins are typically secondary metabolites, produced by organisms in response to external stimuli such as nutritional changes and infection [1,2]. Coumarins occur in all plant parts from roots to flowers and fruits and are found widely spread in various plant families. The present compound has been isolated from the seeds of *Apiumgraveolens* (Umbelliferae), a weed cultivated in several parts of India³. The seeds of this plant are valuable flavouring agents and are widely used in the Ayurvedic and Unani system of medicines for the treatment of bronchitis, asthma, and are also as household remedy for rheumatism [3]. Dried and powdered seeds of *Apium graveolens* were extracted with petroleum ether extract which was chromatographed over a column of silica gel. Elution with ethyl acetate yielded a compound having yellow fluorescence in UV light, crystals from acetone, m.p. 466K. The structure was established on the basis of spectral data: M^+ 262, 1H NMR (200 MHz, $CDCl_3$) δ 1.21 (s, 6H, 2 x $-CH_3$), 1.38 (s, 1H, OH), 3.18 (2H, d, J 8.5Hz, H-3), 4.73 (1H, t, J 8.5Hz, H-3), 6.08 (1H, d, J 9Hz, H-6), 6.67 (1H, s, H-4), 7.45 (1H, d, J 9Hz, H-5). The chemical structure of the title compound is shown in Figure 1.

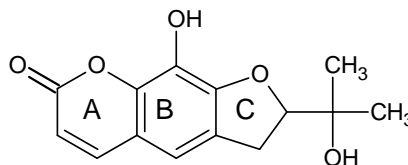


Fig 1: Chemical structure of Rutaretin

2. Experimental Section

A yellow prism crystal of $C_{14}H_{14}O_5 \cdot H_2O$ having approximate dimensions of $0.3 \times 0.3 \times 0.3$ mm was mounted on a Mylar loop. All measurements were made on a Rigaku R-AXIS SPIDER imaging plate area detector with graphite monochromated $Mo-K\alpha$ radiation.

Correspondence
Bandhan Sharma
 Department of Physics, Govt.
 College for Women Parade,
 Jammu. (Autonomous
 College), Jammu and Kashmir,
 India

Indexing was performed from 4 oscillations that were exposed for 90 seconds. The crystal-to-detector distance was 127.40 mm. Cell constants and an orientation matrix for data collection corresponded to a C-centered monoclinic cell with dimensions: $a = 24.6161(8) \text{ \AA}$, $b = 8.1865(3) \text{ \AA}$, $c = 6.6316(2) \text{ \AA}$, $\beta = 103.99(2)^\circ$. The data usually collected using an image plate or CCD camera consists of reflections which runs into several thousands. The intensity data of 14258 reflections were collected in the θ -range (3.17 to 31.97°) of which 2379 were found to be unique (with index range: $-35 \leq h \leq 36$, $-11 \leq k \leq 12$, $-9 \leq l \leq 9$). Based on the distribution of reflections satisfying general and special conditions i.e. $hkl: h+k = 2n$, the space group assigned to the unit cell is C2. Upon refining the reflections using the cut-off criterion, a major chunk of reflections is generally the one whose intensities are very weak and hence are ignored. Therefore, the reflections for which $F_o > 4\sigma(F_o)$ were treated as observed and in the present case, it is 2216. The reflection data were collected for Lorentz and polarization effects. The crystal structure has been solved by direct methods using SHELXS software [4]. The value of $\langle |E^2-1| \rangle$ is fairly good and is an indicator to know whether the full matrix or its principal projections are centric or acentric. The statistical analysis of $ABS(E^2-1)$ in the SHELXS output indicated overall distribution of intensities to be centric. R_{int} and R_{σ} values ($R_{int} = 0.049$ and $R_{\sigma} = 0.036$) indicated

that the intensity data are of good quality. The structure refinement was carried out using SHELXL software [5]. All non-hydrogen atoms of the molecule were obtained from the E-map. The reliability index for the normalized E-value (R_E) comes out to be 0.184. The final refinement yield an R-factor = 0.0356, $wR = 0.0940$. The maximum and minimum residual electron density is 0.41 and -0.28 e \AA^{-3} . Atomic scattering factors were taken from International Tables for Crystallography (1992, Vol. C Tables 4.2.6.87 and 6.1.1.4). The crystallographic data are listed in Table 1.

The three dimensional coordinate data of the title compound has been selected as an input for PASS software to predict the bioactivity relationship [6]. On the basis of x, y, z Coordinates, the molecular structure has been drawn and the bioactivity predictions were determined on the statistics of MNA descriptions for active and inactive fragments. The biological activity spectra for substance have been correlated on Structure Activity Relationships (SAR) data and knowledge SAR base which provides the different P_a (Probability of activity value) and P_i (Probability of inactivity) values. The influence of these description can be positive (if they are found in compounds with particular activity) or negative (if they are found in compounds with particular activity) or even neutral. The possible activity prediction with the value of P_a and P_i are listed in Table 2.

Table 1: Crystal data structure refinement details

Crystal description	Rectangular plates
Empirical formula	$C_{14}H_{16}O_6$
Formula weight	280.27
Temperature (K)	293(2)
Wavelength(\AA)	0.71070 \AA
Unit cell dimensions	
a(\AA)	24.616(8)
b(\AA)	8.1863(3)
c(\AA)	6.632(2)
β ($^\circ$)	103.99(2)
Volume(\AA^3)	1296.78(7)
Z	4
Calculated density(Mg m^{-3})	1.436
F(000)	592
θ -range	3.17 to 31.97°
Index ranges	$-35 \leq h \leq 36$ $-11 \leq k \leq 12$ $-9 \leq l \leq 9$
Refinement method	Full-matrix least-squares on F^2
Data/ restraints/parameters	2379 / 1 / 199
Goodness-of-fit on F^2	1.081
Final R indices	$R_1 = 0.0356$, $WR_2 = 0.0940$
R indices (all data)	$R_1 = 0.0383$, $WR_2 = 0.0955$
Largest diff. peak and hole	0.415 and $-0.285 \text{ e \AA}^{-3}$

Table 2: Possible-activity Predictions

Activity	P_a	P_i
Indanol dehydrogenase	0.195	0.142
Anti-inflammatory	0.673	0.019
Respiratory analeptic	0.658	0.018
Antioxidant	0.521	0.006
Anthelmintic	0.513	0.005
Antiviral	0.517	0.019
Sweetener	0.123	0.121
Antibacterial	0.458	0.021
Nuropeptide Y4	0.276	0.228

3. Results and Discussion

Bond distances and bond angles for non-hydrogen atoms are listed in Table 2. Torsion angles for non-hydrogen are listed in Table 3. An ORTEP view of the molecule indicating the atomic numbering scheme and displacement ellipsoids drawn at 50% probability level is shown in Figure 2 [7]. The geometrical calculations were performed using PARST [8] and PLANTON program [9]. The bond distances and bond angles are in good agreement with the value reported for some analogous structures [10-14].

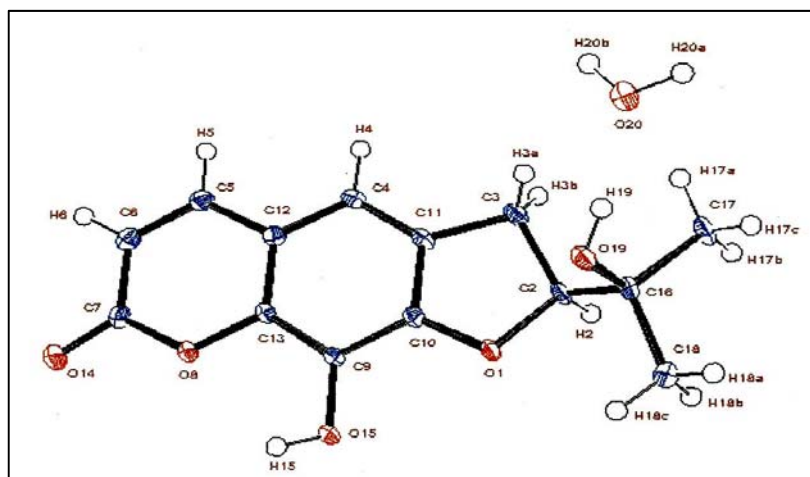


Fig 2: ORTEP view of the molecule indicating atomic numbering scheme and displacement ellipsoids drawn at 50% probability level.

The double bond distances in the lactone moiety i.e. $C7 = O14$ and $C5 = C6$, which are generally responsible for the photoactivity phenomenon in coumarins [12-13]. The pyrone ring A of the molecule is perfectly planar with maximum deviation of $0.008(2)$ Å found for O8. The average value of torsion angles in this ring is $0.89(2)^\circ$. The furan ring exists in 2α -envelope conformation with average value of torsion angles $8.66(2)^\circ$ and the asymmetry bisecting the C10-C11 bond. The oxygen atom [O20] of water molecule acts as proton donor as well as proton acceptor. The donor O20 atom makes the O14 as bifurcated acceptor which is responsible for hydrogen bonded virtual six membered ring as shown in Figure 3. The intermolecular interactions i.e. C18-H18...O1, O20-H20A...O14 and O20-H20B...O14 which are extended parallel through a hydrogen bonded network of the molecules along ab-plane and link one end of the compound whereas the hydrogen interaction O19-H19...O20 link another end of it [15]. The intermolecular O-H... π interaction connects the hydroxyl atom (O15) to the π_1 (comprising of atoms O1, C2, C3, C10 and C11). The molecules linked into chains by a single O15-H15... π hydrogen interaction (Figure 4) in which O15 atom in the

molecule at (x,y,z) acts as a hydrogen-bond donor, via H15, to the ring comprising of atoms O1, C2, C3, C10 and C11 of another molecule at $(-x, y, 2-z)$. This type of edge-to-face $\pi...H$ interaction also supports the supramolecular architect of the Rutaretin. The face to face $\pi... \pi$ stacking interactions link the planar tricyclic moiety with one another and the pack the molecules in reverse orientations as shown in Figure 4. The ring B at (x, y, z) is connected to ring C at $(-x, y, 1-z)$ through $\pi_2... \pi_3$ intermolecular interaction with dihedral angle of 4.37° between them, the interplanar spacing is $3.719(1)$ Å corresponding to offset parameter = 3.095. The ring C is connected to ring B through $\pi... \pi$ intermolecular interactions and it depicts the dimer assembly of the molecules.

The graphical representation of P_a and P_i descriptors depicting the bioactivity is shown in the Figure 5. From the graph it clear that the value of P_a (Probability of activity) is very large as compared to P_i (Probability of inactivity) for Antioxidant, Anti-inflammatory, Antibacterial and Respiratory analeptic which shows the positive influence of these descriptions. For sweetener, the value of P_a and P_i is same which confirms the neutral influence of the descriptor.

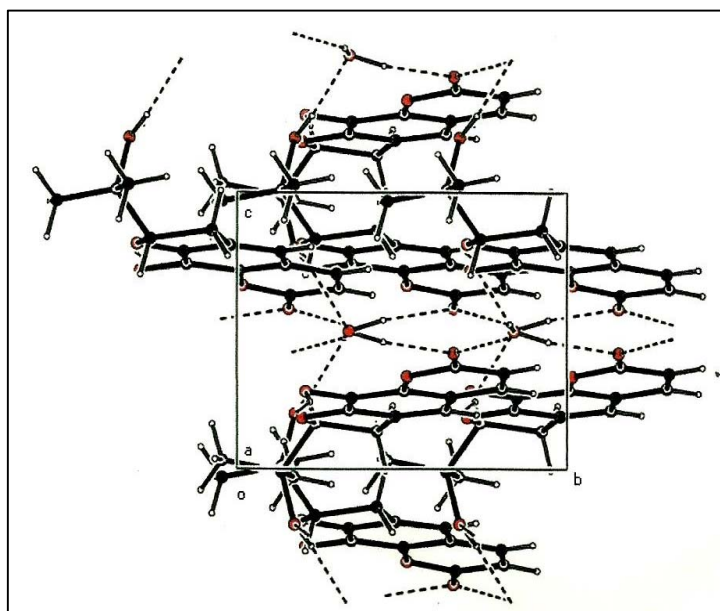


Fig 3: Packing view of the molecules down a-axis depicting the C-H...O and O-H...O hydrogen bonding network.

Table 3: Bond distances (Å) for non-hydrogen atoms (e.s.d.'s in parentheses)

O14-C7	1.229(16)	C12-C4	1.407(17)
O8-C7	1.368(18)	O13-C9	1.402(19)
O8-C13	1.387(15)	C9-C10	1.397(16)
O15-C9	1.355(17)	C10-C11	1.402(19)
O1-C10	1.356(17)	C11-C4	1.373(2)
O1-C2	1.478(15)	C11-C3	1.505(18)
O19-C16	1.438(16)	C3-C2	1.542(2)
C7-C6	1.439(2)	C2-C16	1.532(18)
C6-C5	1.358(2)	C16-C18	1.532(2)
C5-C12	1.429(2)	C16-C17	1.528(17)
C12-C13	1.406(19)		

4. Conclusions

The double bond distances in the lactone moiety i.e. C7 = O14 and C5 = C6 are 1.229(2) and 1.358(2) respectively, which confirms the photoactivity of the title compound as it also observed for other furanocoumarins. The pyrone ring A of the molecule is perfectly planar with maximum deviation of 0.008(2) Å found for O8. The molecules also exhibit C-H...O and O-H...O intermolecular interactions, which shows the stability of the compound. In the Figure 4, the

molecules are linked with edge to face π ...H interactions which supports the supramolecular structure of the title compound and also pack the molecules in reverse orientation i.e. face to face π ... π interactions which also results into the supramolecular structure of the compound. The value of P_a (Probability of activity) is very large as compared to P_i (Probability of inactivity) for Antioxidant, Anti-inflammatory and Respiratory analeptic which shows the positive influence of these descriptions.

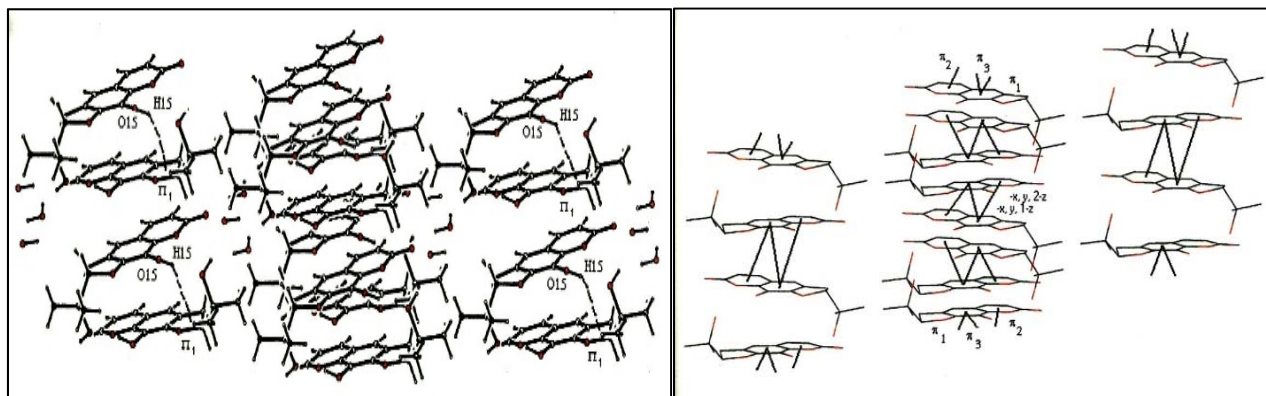


Fig 4: A perspective view of the structures showing the molecules linked into centrosymmetric dimers by O-H... π and π ... π interactions.

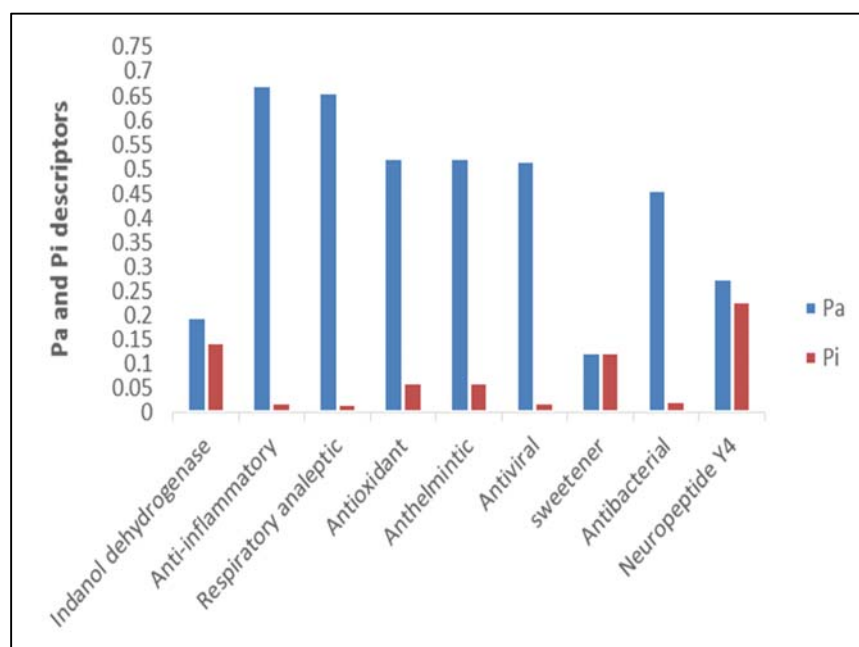


Fig 5: Graphical representation of bioactivity

5. References

1. Cotton CM, Ethnobotany-Principles and Applications, John Wiley & Sons Ltd, Chichester, UK, 1997.
2. Strohl WR, Editorial in Drug Discovery today. 2000; 5:39.
3. Garg SK, Gupta SR, Sharma ND, Phytochemistry. 1978; 17:2135.
4. Sheldrick GM. SHELXS97, Program for crystal structure determination, University of Gottingen, Federal Republic of Germany, 1997.
5. Sheldrick GM. SHELXL97, Program for refinement of crystal structures, University of Gottingen, Federal Republic of Germany, 1997.
6. Poroikov VV, Filimonov DA, Ihlenfeldt WD, Glorizova TA, Lagunin AA, Borodina YV *et al.* J Chem. Inf. Comput. Sci. 2003; 43:228.
7. Farrugia LJ. Applied Crystallography. 1997; 30:659.
8. Nardelli M. J Appl. Crystallography. 1995; 28:659.
9. Spek AL, Acta Crystallography. 2009; C71:3.
10. Sharma B. International Journal of Applied Research. 2016; 2:470.
11. Goswami S, Gupta VK, Sharma A, Gupta BD. Bulletin of material Sciences. 2005; 28:725.
12. Bauri AK, Foro S, Do QNN. Acta Crystallography. 2016; E72:1194.
13. Sharma B. Indian Journal of pure and applied physics, 2015; 53:808.
14. Rajnikant, Dinesh, Shawl AS, Singh TP, Sharma B. Journal of Chemical crystallography. 2005; 35:913.
15. Dseiraju GR, Steiner T. The weak hydrogen bond in structural chemistry and biology, IUCr Oxford Press, New York. 1999; 18.